Chemical Physics Letters 608 (2014) 386–392

Contents lists available at ScienceDirect

Chemical Physics Letters

journal homepage: www.elsevier.com/locate/cplett

Theoretical kinetic study of the unimolecular decomposition of 2-bromopropene

Larisa L.B. Bracco, María P. Badenes, María E. Tucceri *, Carlos J. Cobos

Instituto de Investigaciones Fisicoquímicas Teóricas y Aplicadas (INIFTA), Departamento de Química, Facultad de Ciencias Exactas, Universidad Nacional de La Plata, Casilla de Correo 16, Sucursal 4, 1900 La Plata, Argentina

ARTICLE INFO

Article history:
Received 25 March 2014
In final form 6 June 2014
Available online 14 June 2014

ABSTRACT

The kinetics of the gas phase thermal decomposition of 2-bromopropene at 600–1400 K has been studied by using the unimolecular rate theory combined with different formulations of the density functional theory and high level *ab initio* composite methods. This hydrogen bromide elimination reaction presents two dissociation channels, one forming propyne and another forming allene. High-pressure limit rate coefficients of $(6.2 \pm 1.2) \times 10^{14}$ exp $[-(64.5 \pm 2$ kcal mol$^{-1})/RT]$ and $(1.1 \pm 0.1) \times 10^{14}$ exp $[-(63.6 \pm 2$ kcal mol$^{-1})/RT]$ s^{-1} were obtained for these reaction pathways. The present results allow to elucidate reported contradictory experimental data.

1. Introduction

The contamination of the earth atmosphere is a topic of extreme concern. In particular, it is well known that compounds containing bromine atoms possess a great capacity to damage the ozone layer due to their participation in several catalytic cycles in the stratosphere and troposphere. Because bromine compounds are emitted into the atmosphere mainly from ocean, agriculture, biomass burning, gasoline additives, and from the industry, it is certainly necessary to analyze their environmental impact [1]. For that reason during the last decades experimental and theoretical investigations related to the abundance, profiles and reaction mechanisms of atmospheric bromine compounds, principally bromocarbons, have been reported [2–4].

Special attention has been taken to the hydrogen bromide formation from thermal decomposition of bromine compounds. Particularly, several studies of the gas-phase alkyl bromide decomposition have been reported. However limited information about similar reactions of unsaturated halides is available [5–7]. Concerning 2-bromopropene, which is used as a solvent, as an intermediate for organic synthesis, and as fumigant, only two experimental studies of its thermal decomposition have been reported, and they give contradictory kinetic information. In the first published study, Roy et al. investigated the reaction over the 1100–1250 K temperature range and at total Ar pressures from about 1125–6000 Torr using a single-pulse shock tube technique [8]. They determined an activation energy of 65.2 ± 0.8 kcal mol^{-1} for the global dissociation process (1a) + (1b) and a ratio of 1.8 between the reaction primary products, propyne/allene, that is, a branching ratio for reaction (1a) of $\phi_{1a} = k_{1a}/(k_{1a} + k_{1b}) = 0.64$.

$$CH_2 = CBrCH_3 \rightarrow H_3C - C \equiv CH + HBr \quad (1a)$$

$$CH_2 = CBrCH_3 \rightarrow H_2C = C = CH_2 + HBr. \quad (1b)$$

More recently, Nisar and Awan reinvestigated the reaction in a conventional static system at 571–654 K and at 12–46 Torr of pure 2-bromopropene [9]. A much smaller activation energy of 49.8 ± 1.6 kcal mol^{-1} and a pre-exponential Arrhenius factor of about 20 times smaller were derived, with propyne being the only olefinic product formed ($\phi_{1a} \approx 0.98$). Despite the activation energy differences, the 2-bromopropene follows a first-order kinetic decay in both cases, and only a small pressure effect was observed in the high temperature shock tube experiments [8].

The extrapolation of both sets of experiments leads to differences of about four orders of magnitude for the decomposition rate coefficients of 2-bromopropene within the 571–1250 K range. To clarify this huge discrepancy, a detailed kinetic study of the pressure and temperature dependence of the rate coefficients of reaction (1) and the branching ratio is presented here. To this end, the unimolecular rate theory complemented with molecular information provided by different quantum-chemical methods was employed.

* Corresponding author. Fax: +54 221 4254642.
E-mail address: mtucceri@inifta.unlp.edu.ar (M.E. Tucceri).

http://dx.doi.org/10.1016/j.cplett.2014.06.015
0009-2614/

2. Computational methods

The calculations were performed with the GAUSSIAN 09 program package [10]. The BMK [11], MPWB1K [12], BB1K [13], M05-2X [14] and M06-2X [15] formulations of the density functional theory, DFT, were employed. These models, have been specifically developed for thermochemical kinetic studies, and they give mean absolute deviations from well established experimental activation energies near 1 kcal mol^{-1}. The Pople split-valence triple-ζ basis set 6–311++G(3df,3pd) was used for all DFT calculations. This basis set confers large radial and angular flexibility to represent electron density far from the nuclei and among the bonded atoms, respectively. Additional energy estimates were performed by using high level *ab initio* methods. In particular, the CBS-QB3 Complete Basis Set method [16,17], and the G3B3 [18] and G4 [19] composite models were employed. In all cases, the structural parameters were fully optimized *via* analytic gradient methods. Harmonic vibration frequencies were computed employing analytical second order derivative methods. The Synchronous Transit-Guided Quasi-Newton (STQN) Method was employed for locating transition structures.

3. Results and discussion

3.1. Molecular structures and harmonic vibrational frequencies for the 2-bromopropene and the transition states

The calculated rotational constants and harmonic vibrational frequencies derived from the optimized geometrical parameters of the 2-bromopropene and of the transition states of reactions (1a) (TS-propyne) and (1b) (TS-allene) for each level of theory are listed in Tables 1–3. No general consensus exists for the scaling factors of the here employed DFT approaches with the large 6-311++G(3df,3pd) basis set [20,21]. However, for low frequencies (the more important modes for the present kinetic analysis), scaling factors approaching to the unity have been suggested [20]. Therefore, unscaled vibrational frequencies seem to be appropriate for our study. The obtained bond lengths and bond angles for the 2-bromopropene at the five levels of theory differ, respectively, among themselves in only ±0.02 Å and ±0.4° and are in good agreement with previous studies [22]. For the sake of simplicity, in Figure 1 only averaged bond lengths and bond angles are reported. A very good agreement between these and reported experimental values was found [23].

As Table 1 indicates, for the calculated harmonic vibrational frequencies of 2-bromopropene differences up to 69 cm^{-1} were found among the five models employed and they are in reasonable agreement with the experimentally determined values [24]. Table 1 also includes mode assignments estimated from the animation of the normal modes. However, due to some modes being strongly coupled, these assignments should be considered only approximate.

Four-center transition state structures for the TS-propyne and TS-allene were determined at all employed levels of theory. A normal mode analysis led to only one imaginary frequency indicating the presence of true transitions states. The geometrical parameters for TS-propyne differ in about ±0.1 Å and ±35.3° among employed levels of theory, whereas for TS-allene the differences are ±0.1 Å and ±21.9°. The individual rotational constants are given in Tables 2 and 3. The average structures of both transition states are depicted in Figure 1. These geometries resemble the recently obtained for the transition states in the thermal decomposition of 2-chloropropene [25]. The resulting harmonic vibrational frequencies for TS-propyne and TS-allene are consigned in Tables 2 and 3. Deviations smaller of about 100 cm^{-1}, mainly for the highest vibrational modes, are observed.

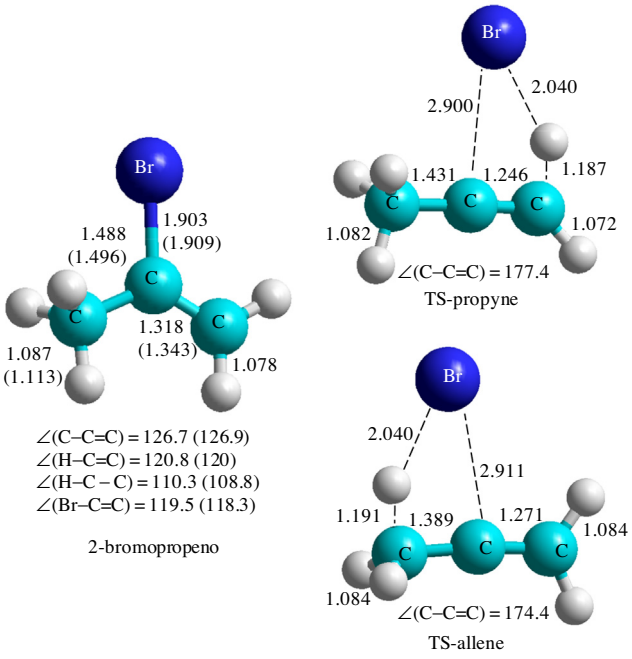

Figure 1. Average geometrical structures (bond distances in Å, bond angles in degree) of 2-bromopropene, TS-propyne, and TS-allene. Experimental values from Ref. [23] are given between parenthesis.

3.2. Energetics of reaction (1)

To estimate the enthalpy changes for the decomposition channels (1a) and (1b), the standard enthalpy of formation at 298 K, $\Delta H_{f,298}$, for 2-bromopropene was first determined. To this end, we used the following working reactions,

$$CH_2=CHBr + CH_3CH_3 \rightarrow CH_2=CBrCH_3 + CH_4 \quad (2)$$

$$CH_3CH_2Br + CH_2=CH_2 \rightarrow CH_2=CBrCH_3 + CH_4 \quad (3)$$

In these isodesmic and isogyric processes, the number of each type of bonds in reactants and products and the spin multiplicities are conserved [26]. To derive $\Delta H_{f,298}$, recommended experimental enthalpies of formation at 298 K (in kcal mol^{-1}) for CH_2=CHBr (18.9 ± 0.5), CH_3CH_3 (−20.04 ± 0.07), CH_4 (−17.818 ± 0.014), CH_3CH_2Br (−14.70 ± 0.24) and CH_2=CH_2 (12.5 ± 0.1) were employed [27]. The resulting average $\Delta H_{f,298}$ values for 2-bromopropene (in kcal mol^{-1}) are: 9.3 (BMK), 9.2 (mPWB1K), 9.3 (BB1K), 9.3 (M05-2X), 9.2 (M06-2X), 9.3 (CBS-QB3), 8.5 (G3B3), and 8.3 (G4). To our knowledge, the only estimation reported for this molecule is *ca.*7 kcal mol^{-1} [28]. On the basis of the accurate CBS-QB3, G3B3 and G4 GAUSSIAN models, a recommend value of $\Delta H_{f,298}$ = 8.7 ± 1.3 kcal mol^{-1} for 2-bromopropene is proposed.

Table 4 shows the enthalpies for the reactions pathways (1a) and (1b) estimated using the above $\Delta H_{f,298}$ value and the enthalpy of formation of −8.67 ± 0.042, 44.2 ± 0.2 and 45.5 ± 0.3 kcal mol^{-1} for HBr, H_3C—C≡CH, and H_2C=C=CH_2, respectively [27]. In addition, reaction enthalpies calculated, in a direct way, from total electronic energies corrected for zero-point energies are presented in Table 4. As can be seen, both are endothermic processes, reaction (1a) in about 26.5 kcal mol^{-1} and (1b) in about 27.8 kcal mol^{-1}.

The computed DFT and *ab initio* electronic energy barriers at 0 K, $\Delta H_0^{\#}$, connecting the 2-bromopropene with the products for both reaction channels are given in Table 4. As aforementioned, a chemical accuracy of about 1 kcal mol^{-1} is expected for these calculations. The calculations predict four-center transition states (see

Table 1
Harmonic vibrational frequencies (in cm^{-1}), approximate assignments, infrared intensities (in km mol^{-1}), and rotational constants (in cm^{-1}) calculated at different levels of theory for 2-bromopropene.

Property	BMK	mPWB1K	BB1K	M05-2X	M06-2X	Average	Exp. [24]
Vibrational frequencies							
Stretching asym. CH_2	3255 (0.3)	3322 (1)	3315 (1)	3302 (0.3)	3264 (0.3)	3292	3115
Stretching sym. CH_2	3155 (1)	3220 (2)	3213 (2)	3200 (1)	3161 (1)	3190	3010
Stretching asym. CH_3	3134(7)	3196 (11)	3190 (11)	3170 (7)	3142 (6)	3166	2987
Stretching asym. CH_3	3110 (2)	3179 (5)	3172 (5)	3159 (3)	3135 (3)	3151	2930
Stretching sym. CH_3	3042 (7)	3106 (11)	3100 (11)	3090 (8)	3060 (8)	3080	
Stretching C=C	1705 (45)	1765 (46)	1760 (46)	1736 (46)	1723 (42)	1738	1640
Bending CH_2 (CH_3)	1511 (10)	1510 (10)	1508 (10)	1510 (11)	1495 (10)	1507	1443
Bending CH_2 (CH_3)	1496 (11)	1492 (12)	1489 (12)	1495 (12)	1480 (11)	1490	1439
Bending CH_2	1452 (0.1)	1461 (0.4)	1458 (0.4)	1452 (0.7)	1440 (0.3)	1453	1405
Umbrella CH_3	1416 (7)	1427 (9)	1425 (9)	1425 (10)	1412 (8)	1421	1379
Stretching CBr	1201 (69)	1216 (67)	1212 (68)	1199 (71)	1197 (67)	1205	1170
Bending CH_2 (CH_3)	1081(0.00)	1088 (0.00)	1085 (0.00)	1090 (0.05)	1080 (0.00)	1085	1045
Bending CCH (CH_3)	1018 (0.7)	1032 (0.8)	1029 (0.8)	1032 (0.6)	1026 (0.5)	1027	996
Wagging CH_2	951 (45)	962 (2)	959 (2)	954 (44)	952 (41)	956	925
Bending CCH (CH_2)	946 (4)	957 (43)	954 (43)	949 (2)	947 (2)	951	883
Rocking CH_2	723(0.04)	721 (0.3)	719 (0.3)	718 (0.4)	721 (0.5)	720	
Bending CCC	577 (23)	581 (23)	578 (24)	560 (28)	574 (24)	574	551
C2 out of plane	434 (9)	439 (9)	438 (9)	433 (9)	442 (8)	437	414
Bending CCBr	362 (0.2)	362 (0.3)	361 (0.3)	360 (0.3)	365 (0.2)	362	335
Bending CCBr	306 (0.9)	303 (0.8)	302 (0.8)	308 (1)	312 (0.9)	306	301
Torsion	238 (0.2)	210 (0.2)	210 (0.2)	214 (0.3)	244 (0.3)	223	196
Rotational constants							
A	0.310	0.315	0.316	0.312	0.312	0.313	
B	0.103	0.106	0.106	0.105	0.105	0.105	
C	0.079	0.081	0.081	0.080	0.080	0.080	

Table 2
Harmonic vibrational frequencies (in cm^{-1}), approximate assignments, and rotational constants (in cm^{-1}) calculated at different levels of theory for TS-propyne.

Property	BMK	mPWB1K	BB1K	M05-2X	M06-2X	Average
Vibrational frequencies						
Stretching CH (CH_2)	3271	3368	3358	3348	3295	3328
Stretching asym. CH_3	3164	3227	3220	3188	3161	3192
Stretching asym. CH_3	3114	3177	3170	3142	3114	3143
Stretching sym. CH_3	3008	3063	3056	3036	3010	3035
Stretching C≡C	2045	2079	2071	2047	2053	2059
Stretching CC	1859	1807	1802	1780	1819	1814
Bending CH_2 (CH_3)	1476	1485	1482	1488	1464	1479
Bending CH_2 (CH_3)	1438	1436	1434	1432	1415	1431
Umbrella CH_3	1397	1399	1396	1394	1375	1392
Stretching BrH	1063i	1162i	1161i	1219i	1122i	1145i
Wagging CH_2 (CH_3)	1064	1066	1064	1068	1050	1063
Bending CH_2	1060	1044	1043	1027	1046	1044
Bending CCH	1021	1015	1014	1005	1002	1011
Wagging CH_2	881	877	876	866	861	891
Bending CCH	869	860	862	850	848	861
Rocking CH_2	547	528	527	513	519	526
Bending CCC	522	505	510	502	508	509
C out of plane	333	341	340	336	333	337
Stretching BrH	253	253	253	261	278	259
Torsion C-CH_3	190	194	195	187	182	189
Stretching CBr	132	136	135	142	145	138
Rotational constants						
A	0.2892	0.2902	0.2904	0.2861	0.2855	0.2883
B	0.0680	0.0718	0.0714	0.0718	0.0716	0.0709
C	0.0556	0.0582	0.0579	0.0581	0.0579	0.0576

Figure 1) located at 59–65 kcal mol^{-1} above the 2-bromopropene molecule. In particular, the specific DFT methods led to average $\Delta H_0^{\#}$ values of 60.8 and 60.3 kcal mol^{-1} for channels (1a) and (1b), respectively. The *ab initio* composite methods predict larger values of 64.0 and 64.3 kcal mol^{-1}. Although the employed DFT models have been more systematically validated against well known experimental barriers than the employed *ab initio* models, which have chemical accuracy for thermochemistry, no conclusive choice between the two sets of $\Delta H_0^{\#}$ values can be advanced. Therefore, the average of all data seems to be a reasonable election: $\Delta H_0^{\#}$ = 62.0 kcal mol^{-1} (reaction (1a)) and $\Delta H_0^{\#}$ = 61.8 kcal mol^{-1} (reaction (1b)). From the scatter of the calculated values, a conservative uncertainty of ±2 kcal mol^{-1} seems to be reasonable for the electronic energy barriers.

The large G4 value, 78.7 kcal mol^{-1}, computed for the reaction enthalpy of the $CH_2 = CBrCH3 \rightarrow H_2C = CCH_3 + Br$ reaction channel at 0 K indicates that, at the studied temperatures, this process does not play a role.

Table 3
Harmonic vibrational frequencies (in cm^{-1}), approximate assignments, and rotational constants (in cm^{-1}) calculated at different levels of theory for TS-allene.

Property	BMK	mPWB1K	BB1K	M05-2X	M06-2X	Average
Vibrational frequencies						
Stretching CH (CH_3)	3261	3326	3319	3279	3239	3285
Stretching CH (CH_3)	3186	3254	3246	3223	3187	3219
Stretching asym. CH_2	3117	3176	3169	3148	3116	3145
Stretching sym. CH_3 and CH_2	3094	3159	3152	3132	3094	3126
Stretching C=C	1975	2030	2025	2003	2002	2007
Stretching CBr	1704	1715	1710	1673	1712	1703
Bending CCH	1450	1463	1460	1464	1441	1456
Bending CH_2	1340	1358	1357	1346	1336	1348
Stretching CH (CH_2 and CH_3)	1309	1286	1286	1283	1276	1288
Stretching BrH	1203	1203	1201	1187	1203	1200
Stretching BrH	1128i	1140i	1140i	1222i	1120i	1150i
Bending CCH	1052	1055	1052	1056	1039	1051
Stretching CC	986	995	994	991	978	989
Bending CCH	893	905	904	894	889	897
C out of plane (CH_2)	885	901	897	894	875	890
Bending CCH	545	545	542	530	530	538
Deformation	523	536	537	514	513	525
C out of plane	346	351	350	348	346	348
Wagging CH_2	246	249	250	240	263	250
Bending HCC	233	218	219	177	175	204
Deformation	159	167	165	173	174	168
Rotational constants						
A	0.290	0.294	0.293	0.290	0.289	0.291
B	0.068	0.071	0.070	0.071	0.070	0.070
C	0.055	0.058	0.057	0.057	0.057	0.057

Table 4
Enthalpies for the thermal decomposition of 2-bromopropene (in kcal mol^{-1}) ΔH_r, electronic energy barriers at 0 K $\Delta H_0^{\#}$ (in kcal mol^{-1}), preexponential factors A_∞ (in s^{-1}), and activation energies $E_{a,\infty}$ (in kcal mol^{-1}) for channels (1a) and (1b) calculated at different levels of theory.

Level of theory	ΔH_r			$\Delta H_0^{\#}$	$E_{a,\infty}$	A_∞
	Isodesmic 298 K	Direct				
		0 K	298 K			
CH_2=$CBrCH_3$ → H_3C–C≡CH + HBr						
M05-2X	26.3	28.9	30.4	59.4	61.9	5.7×10^{14}
M06-2X	26.3	26.9	28.4	60.3	63.4	9.7×10^{14}
BMK	26.3	28.5	30.0	62.0	64.4	5.9×10^{14}
BB1K	26.2	27.0	28.4	60.8	63.3	5.3×10^{14}
mPWB1K	26.3	28.1	29.5	61.3	63.8	5.3×10^{14}
CBS-QB3	26.2	26.8	28.2	63.5	65.7	5.2×10^{14}
G3B3	27.0	27.0	28.5	64.2	66.4	6.3×10^{14}
G4	27.3	27.2	28.7	64.4	66.8	6.3×10^{14}
CH_2=$CBrCH_3$ → H_2C=C=CH_2 + HBr						
M05-2X	27.6	27.9	29.3	58.8	60.8	1.3×10^{14}
M06-2X	27.6	26.9	28.3	60.2	62.0	1.3×10^{14}
BMK	27.6	27.2	28.6	61.3	63.2	1.1×10^{14}
BB1K	27.5	25.8	27.2	60.3	62.2	1.0×10^{14}
mPWB1K	27.6	27.4	28.6	60.7	62.8	1.2×10^{14}
CBS-QB3	27.5	27.7	29.0	63.7	65.4	9.3×10^{13}
G3B3	28.3	28.0	29.3	64.5	66.1	8.9×10^{13}
G4	28.6	28.3	29.6	64.7	66.5	1.1×10^{14}

3.3. Theoretical kinetic analysis

3.3.1. Limiting high pressure rate coefficients

The limiting high pressure rate coefficient for this tight reaction, k_∞, was calculated using the canonical formulation of the transition state theory. To overlap the kinetic data of Roy et al. [8] with those of Nisar and Awan [9] k_∞ was calculated between 600 and 1400 K at each level of theory. The vibrational and rotational partition functions were evaluated using the molecular input data obtained from the quantum-chemical calculations (Tables 1–3). The partition functions for the internal rotational motions, for the parent and the transition states, were estimated using the Troe's formalism [29]. In this approach, the partition function for a hindered rotor is obtained from a suitable interpolation between the free rotor and torsion partition functions. The CH_3 moiety of the 2-bromopropene was considered as a hindered rotor with a barrier height of 2.7 kcal mol^{-1} and a reduced moment of inertia of 3.1 amu $Å^2$ [30,31]. For the TS-propyne values of 1.8 kcal mol^{-1} and 3.2 amu $Å^2$ were estimated for these properties. However, at the studied temperatures both internal rotations are almost free. On the other hand, TS-allene probably exhibits a rigid structure which avoids the internal rotation.

The obtained rate coefficients at all quantum-chemical levels are given in Table S1 of the Supplementary content.

Over the studied temperature range a strict Arrhenius behavior for k_∞ was observed. The plots for each level of theory are shown in Figures S1 and S2 of the Supplementary content. The obtained activation energies $E_{a,\infty}$ and pre-exponential factors A_∞ are listed in Table 4. An inspection of this table shows that all calculated $E_{a,\infty}$ are considerably higher than the measured by Nissar and Awan [9] of 49.8 ± 1.6 kcal mol^{-1}. However, they are close to the activation energy reported by Roy et al. [8] of 65.2 ± 0.8 kcal mol^{-1}. In fact, this value lies between those predicted for reaction (1a) by the DFT, 63.4 kcal mol^{-1}, and the *ab initio*, 66.3 kcal mol^{-1} models. The value obtained from all calculations of 64.5 ± 2 kcal mol^{-1} agrees very well with the experimental. As Table 4 shows, similar A_∞ values are predicted by most theoretical methods. Therefore, the averaged Arrhenius Eq. (4) is proposed to represent reaction (1a) between 600 and 1400 K,

$$k_\infty(1a) = (6.2 \pm 1.2) \times 10^{14} \exp\,[-(64.5 \pm 2 \text{ kcal mol}^{-1})/RT]\ s^{-1}. \quad (4)$$

This expression is in very good agreement with the reported by Roy et al., after a correction by $\phi_{1a} = 0.64$, of $(5.3 \pm 3) \times 10^{14}$ exp [−(65.2 ± 0.8 kcal mol^{-1})/RT] s^{-1} [8]. However, it is in strong disagreement with the obtained by Nisar and Awan in a static system of $(3.0 \pm 6) \times 10^{13}$ exp [−(49.8 ± 1.6 kcal mol^{-1})/RT] s^{-1} [9].

In a similar way, the equation predicted for channel (1b) is

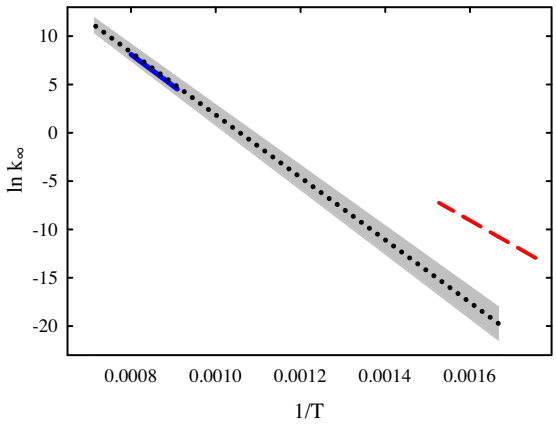

Figure 2. Temperature dependence of the high pressure rate coefficients (in s^{-1}). Solid line: experimental results from Ref. [8]; dashed line: experimental data from Ref. [9]; dotted line: theoretical estimation from the averaged Arrhenius equations (this work); shaded area: range of results considering the inherent uncertainty in the estimation of the electronic energy barriers of ±2 kcal mol^{-1}.

$$k_\infty(1b) = (1.1 \pm 0.1) \times 10^{14} \exp[-(63.6 \pm 2 \text{ kcal mol}^{-1})/RT] \text{ s}^{-1}. \quad (5)$$

Arrhenius plots for the experimental and the present result are depicted in Figure 2. The shaded area shows the rate coefficients range obtained with the estimated uncertainty of ±2 kcal mol^{-1} (see Section 3.2) in the activation energies. The Arrhenius plots derived for each quantum-chemical method are given in the Supplementary Content.

For the sake of consistency, the results presented above were derived using the average of the calculated frequencies for 2-bromopropene and for the respective transitions states. However, if the experimental values for the frequencies of 2-bromopropene are used in the estimation of k_∞, the obtained results become a factor of about 1.5 smaller, in better agreement with the rate coefficients determined by Roy et al. [8].

It is important to note (Table 4) that, despite the similarity of the activation energy values, the differences in A_∞ between the two reaction paths can be attributed to the difference in the internal methyl rotor of the two transitions states, which is highly hindered in the case of the TS-allene but corresponds to nearly free rotation in the TS-propyene.

3.3.2. Limiting low pressure rate coefficients

The experimental evidence indicates that the rate coefficients determined for the 2-bromopropene unimolecular reaction are very close to the high pressure limit, under the studied pressure and temperature conditions [8,9]. In addition, the branching ratio value for $H_3C{-}C{\equiv}CH$ formation is 0.64 according to Ref. [2] or higher than 0.98 [9]. However, to extend the exploration to the fall-off region, an estimation of the value for the low pressure rate coefficient, k_0, is mandatory. At the theoretical level, k_0 can be conveniently represented by the product of the strong collision rate coefficient k_0^{SC} and the weak collision efficiency β_c [29]. The relevant terms contributing to k_0^{SC} are explicitly accounted for by the specific factors of Eq. (6).

$$k_0 = \beta_c \text{ [M] } Z_{LJ} \text{ } (\rho_{vib,h}(E_0) \text{ k T}/Q_{vib}) \text{ } \exp(-E_0/\text{k T}) \text{ } F_{anh} \text{ } F_E \text{ } F_{rot} \text{ } F_{rotint} \quad (6)$$

All these factors were calculated employing the average molecular parameters listed in Tables 1–3. In the following we will present values for the channel (1a). Here $\rho_{vib,h}(E_0) = 1.36 \times 10^{10}$ $(\text{kcal mol}^{-1})^{-1}$ is the harmonic vibrational density of states of 2-bromopropene at the threshold dissociation energy $E_0 \approx \Delta H_0^{\#} = 62.0$ kcal mol^{-1} (see Section 3.3.1). Anharmonic corrections are accounted for by $F_{anh} = 1.13$. The rest of the factors were calculated at 600 and 1200 K (indicated in brackets). $Q_{vib} = 14.8$ (1.17 $\times 10^3$) is the vibrational partition functions of 2-bromopropene; $F_E = 1.30$ (1.82) corrects $\rho_{vib,h}(E_0)$ by the spread of internal energies; tight external rotations are taken into account in $F_{rot} = 2.70$ (1.72) and values of $F_{rotint} = 3.51$ (1.60) were calculated for the internal rotation factor. The Lennard–Jones collision frequencies Z_{LJ} were calculated using estimated parameters of $\sigma = 5.3$ Å and $\varepsilon/k = 390$ K for 2-bromopropene, and recommended values of 3.465 Å and 110.5 K for Ar diluent [32]. Z_{LJ} values of 5.09×10^{-10} cm^3 $molecule^{-1}$ s^{-1} for M = 2-bromopropene at 600 K, and of 5.08×10^{-10} cm^3 $molecule^{-1}$ s^{-1} for M = Ar at 1200 K were calculated. To account for weak collisions, reasonable β_c values of 0.4 for 2-bromopropene and 0.1 for Ar were employed. Then, the values $k_0 = 8.2 \times 10^{-23}$ [2-bromopropene] at 600 K and $k_0 = 4.1 \times 10^{-14}$ [Ar] cm^3 $molecule^{-1}$ s^{-1} at 1200 K were obtained for reaction (1a). In a similar way, for reaction (1b) the values $k_0 = 9.3 \times 10^{-23}$ [2-bromopropene] at 600 K and $k_0 = 4.3 \times 10^{-14}$ [Ar] cm^3 $molecule^{-1}$ s^{-1} at 1200 K were predicted.

Due to partial compensation between the more important factors $\rho_{vib,h}$ and Q_{vib} in Eq. (6), no changes are observed when employing the experimental frequencies for 2-bromopropene.

3.3.3. Falloff curves

The pressure dependence of the rate coefficients of a dissociation reaction depends on the complex interplay established between the intermolecular (collisional) and intramolecular (unimolecular) processes. In the present study, Troe's double reduced method was employed to predict the falloff curve of 2-bromopropene decomposition reaction [33]. For this, the relative rate coefficients k/k_∞ were estimated by using the general expression

$$k/k_\infty = [x/(1+x)]F(x) \quad (7)$$

Here, the pressure dependence is expressed by $x = k_0/k_\infty$. The term between brackets in Eq. (7) corresponds to the Lindemann–Hinshelwood mechanism, while the factor $F(x)$ accounts for corrections due to the energy and total angular momentum dependence of the energized molecules and for the multistep character of the collisional energy transfer. The well known formulation of Ref. [34] and a recent approach for $F(x)$ that explicitly accounts for cases where the broadening of the falloff curves is particularly pronounced (when the center broadening factor $F_{cent} = F(x = 1)$ is below about 0.4) were employed [35]. In this last formulation, $F(x)$ is given by

$$F(x) = (1 + x/x_0)/[1 + (x/x_0)^n]^{1/n}. \quad (8)$$

In Eq. (8), $n = [\ln 2/\ln(2/F_{cent})][1 - b + b(x/x_0)^q]$; $q = (F_{cent} - 1)/\ln(F_{cent}/10)$; $x_0 = 1$ and $b = 0.2$. F_{cent} is approximated as $F_{cent} \approx F_{cent}^{WC} F_{cent}^{SC}$, where F_{cent}^{SC} is the strong collision broadening factor [36] and $F_{cent}^{WC} \approx \beta_c^{0.14}$ is the weak collision broadening factor [34]. This new formulation has been successfully employed in thermal decomposition studies of the C_2F_4 [35,37], C_3F_6 [38] and cyclic C_3F_6 [39] molecules.

To calculate F_{cent} the above enthalpies and vibrational frequencies for the transition states and the estimated weak collision efficiencies were used. In this way, similar F_{cent} values of 0.25 and 0.14 were calculated at 600 and 1200 K for both reaction channels. As in previous studies [37–39], reaction (1) exhibits small F_{cent} values and, thus, the falloff approach of Ref. [35] is especially appropriate. The experimental data and the reduced falloff curves derived from the two models [34,35] for the channel (1a) are depicted in Figure 3. The data of Roy et al. [8] are the result of a modeling simulation performed at about 1200 K with an average energy transferred in up collisions of 1000 cm^{-1} (equivalent to $\beta_c \approx 0.3$), and

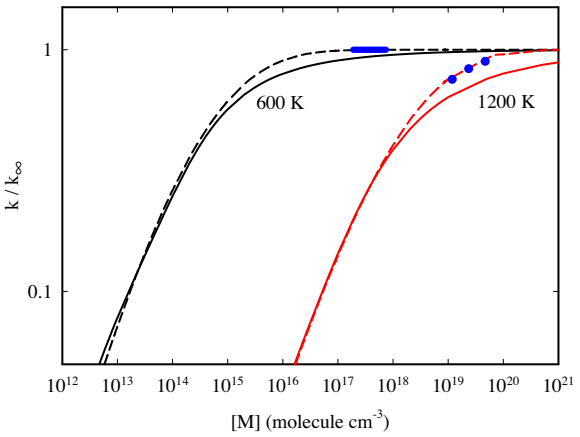

Figure 3. Reduced falloff curves for decomposition of 2-bromopropene at 600 K and at 1200 K for the channel (1a). [M] = [2-bromopropene] at 600 K and [M] = [Ar] at 1200 K. Solid line correspond to formulation of Ref. [34] and dashed line is the derived from approach of Ref. [35]. Filled circles: Ref. [8], thick line: Ref. [9].

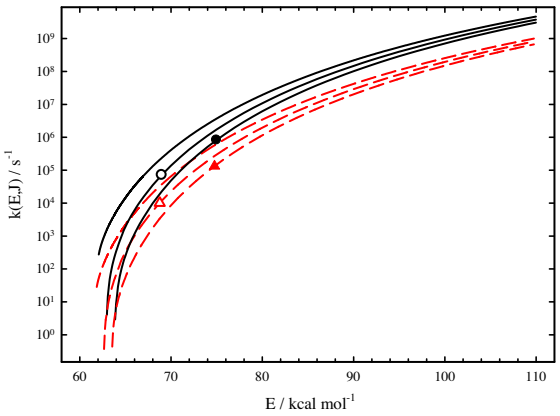

Figure 4. Specific rate coefficients k(E,J) for 2-bromopropene decomposition for $J = 0$, 72, and 102 (from top to bottom). Solid line: channel (1a); dashed line: channel (1b). Filled circle: $E = 75$ kcal mol^{-1} and $J = 102$ (channel (1a), 1200 K); opened circle: $E = 69$ kcal mol^{-1} and $J = 72$ (channel (1a), 600 K); filled triangle: $E = 75$ kcal mol^{-1} and $J = 102$ (channel (1b), 1200 K); opened triangle: $E = 69$ kcal mol^{-1} and $J = 72$ (channel (1b), 600 K).

lie within the experimental error limits of about 20%. The present results clearly indicate that under the experimental conditions reaction (1) is in the high part of the falloff curve, very close to the high pressure limit. In addition, our simulation shows that the low temperature experiments of Nisar and Awan [9] are also very close to the high pressure region. However, the low values derived for both Arrhenius parameters (see Section 3.3.1) largely disagree with those obtained by Roy et al. and with the present simulation of the reaction.

Similar falloff curves were derived from the two employed approach for the channel (1b) but they are left shifted, approximately, by a factor of 3 at 600 K and of 4 at 1200 K.

3.3.4. Branching ratio

Specific rate coefficients $k(E,J)$ resolved in the total energy E and total angular momentum quantum number J were calculated using the Rice–Ramsperger–Kassel-Marcus (RRKM) theory, $k(E,J) = W(E,J)/h\rho(E,J)$ [40]. Here, $W(E,J)$ is the sum of rovibrational levels of the transition state and $\rho(E,J)$ the rovibrational density of states of the decomposed molecule. The molecular input data listed in Tables 1–3 were employed in these calculations together with the average electronic energy barriers derived in Section 3.2. $W(E,J)$ and $\rho(E,J)$ were evaluated by direct state counting using the Bayer–Swinehart algorithm [41] and active K rotational quantum numbers for both the 2-bromopropene and the transition state were assumed. The resulting $k(E,J)$ for both reaction channels are given in Figure 4. Using average values of $E = 69$ kcal mol^{-1} and $J = 72$ derived from a Boltzmann distribution at 600 K, average specific rate coefficients of 7.2×10^4 s^{-1} for channel (1a) and 1.0×10^4 s^{-1} for channel (1b), were calculated. In a similar way, at 1200 K, from estimated values of $E = 75$ kcal mol^{-1} and $J = 102$, the specific rate coefficients 8.2×10^5 s^{-1} for channel (1a) and 1.3×10^5 s^{-1} for channel (1b) were computed. From these values, an almost temperature independent $\phi_{1a} \approx 0.87$ results.

On the other hand, E-resolved specific rate coefficients were estimated using the inverse Laplace transform method, $k(E) = A_\infty \rho(E - E_{a,\infty})/\rho(E)$ [42]. As in recent studies [35,43] we used this method to derive $k(E)$ employing the Whitten–Rabinovitch approximation for the density of states [44]. From the Arrhenius parameters of Eq. (4) and (5), $k(E)$ values at 600 and 1200 K were calculated. The resulting values of 8.2×10^4 s^{-1} for channel (1a) and 2.8×10^4 s^{-1} for channel (1b) at 600 K, and 2.3×10^6 s^{-1} for channel (1a) and 6.3×10^5 s^{-1} for channel (1b) at 1200 K were obtained. From these data, ϕ_{1a} values of 0.75 and 0.78 were respectively estimated.

Finally, the pressure dependence of ϕ_{1a} at 600 and 1200 K was studied. For this, the above k_0 and k_∞ rate coefficients were used. Branching ratio values for reaction (1a) of 0.47 and 0.49 were calculated at 600 and 1200 K at the low pressure limit, and of 0.73 and 0.79 at the high pressure limit. The present calculations, in agreement with the experimental results from Ref. [8] and [9], demonstrate that the thermal decomposition of 2-bromopropene proceeds predominantly through the channel (1a) at the high pressure regime. In addition, they show the role that intermolecular and intramolecular processes play on the efficiency of the formed products.

4. Conclusions

The present quantum-mechanical and kinetic study allows to elucidate contradictory results in the gas-phase thermal decomposition of 2-bromopropene. The theoretical Arrhenius parameters obtained for the high pressure limit rate coefficients for the predominant reaction channel forming HBr and propyne, support those determined by Roy et al. [8]. However, they are in strong disagreement with those reported by Nisar and Awan [9]. The reason for the large discrepancy found between the kinetic data of both studies remains still unclear.

Acknowledgements

This research project was supported by the Universidad Nacional de La Plata, the Consejo Nacional de Investigaciones Científicas y Técnicas (CONICET), and the Agencia Nacional de Promoción Científica y Tecnológica.

Appendix A. Supplementary data

Supplementary data associated with this article can be found, in the online version, at http://dx.doi.org/10.1016/j.cplett.2014.06.015.

References

[1] The Handbook of Environmental Chemistry, in: P. Fabian, O.N. Singh (Eds.), Reactive Halogen Compounds in the Atmosphere, vol. 4, Springer-Verlag, Berlin, Heidelberg, 1999.
[2] A. Kerkweg, P. J'ockel, N. Warwick, S. Gebhardt, C.A.M. Brenninkmeijer, J. Lelieveld, Atmos. Chem. Phys. 8 (2008) 5919.

[3] S. Raimund et al., Biogeosciences 8 (2011) 1551.
[4] R. Hossaini et al., Atmos. Chem. Phys. 13 (2013) 11819.
[5] A. Maccoll, Chem. Rev. 69 (1969) 33.
[6] S.W. Benson, H.E. O'Neal, Kinetic Data on Gas Phase Unimolecular Reactions, NSRDS-NBS, 1970.
[7] NIST Chemical Kinetics Database Standard Reference Database 17, Version 7.0 (Web Version), Release 1.6.3 Data Version 2011.06, 2011.
[8] K. Roy, I.A. Awan, J.A. Manion, W. Tsang, Phys. Chem. Chem. Phys. 5 (2003) 1086.
[9] J. Nisar, I.A. Awan, Int. J. Chem. Kinet. 39 (2007) 1.
[10] M.J. Frisch et al., Gaussian 09, Revision A.02, Gaussian, Inc., Pittsburgh, PA, 2009.
[11] A.D. Boese, J.M.L. Martin, J. Chem. Phys. 121 (2004) 3405.
[12] Y. Zhao, D.G. Truhlar, J. Phys. Chem. A 108 (2004) 6908.
[13] Y. Zhao, B.J. Lynch, D.G. Truhlar, J. Phys. Chem. A 108 (2004) 2715.
[14] Y. Zhao, N.E. Schultz, D.G. Truhlar, J. Chem. Theory Comput. 2 (2006) 364.
[15] Y. Zhao, D.G. Truhlar, Theor. Chem. Acc. 120 (2008) 215.
[16] J.A. Montgomery Jr., M.J. Frisch, J.W. Ochterski, G.A. Petersson, J. Chem. Phys. 110 (1999) 2822.
[17] J.A. Montgomery Jr., M.J. Frisch, J.W. Ochterski, G.A. Petersson, J. Chem. Phys. 112 (2000) 6532.
[18] A.G. Baboul, L.A. Curtiss, P.C. Redfern, K.L. Raghavachari, J. Chem. Phys. 110 (1999) 7650.
[19] L.A. Curtiss, P.C. Redfern, K.L. Raghavachari, J. Chem. Phys. 126 (2007) 084108.
[20] J.P. Merrick, D. Moran, L. Radom, J. Phys. Chem. A 111 (2007) 11683.
[21] I.M. Alecu, J. Chem. Theory Comput. 6 (2010) 2872.
[22] L. Mina, S.K. Myung, J. Chem. Phys. 119 (2003) 12351.
[23] R.L. Hilderbrandt, S.H. Schei, J. Mol. Struct. 118 (1984) 11.
[24] R. Meyer, Hs.H. Günthard, Spectrochim. Acta Part A 23 (1967) 2341.
[25] M.E. Tucceri, M.P. Badenes, C.J. Cobos, J. Phys. Chem. A 117 (2013) 10218.
[26] W.J. Hehre, L. Radom, P.v.R. Schleyer, J.A. Pople, Ab Initio Molecular Orbital Theory, Wiley, New York, 1986.
[27] S.P. Sander et al., Chemical Kinetics and Photochemical Data for Use in Atmospheric Studies, NASA/JPL Data Evaluation, Evaluation No. 17, JPL Publication 06-2, NASA, Pasadena, CA, 2011. <http://jpldataeval.jpl.nasa.gov>.
[28] A.C. Deakyne et al., Croat. Chem. Acta 82 (2009) 165.
[29] J. Troe, J. Chem. Phys. 66 (1977) 4758.
[30] H.P. Benz, A. Bauder, J. Mol. Spectrosc. 21 (1966) 165.
[31] S. Bell, G.A. Guirgis, A.R. Fanning, J.R. Durig, J. Mol. Struct. 178 (1988) 63.
[32] F.M. Mourits, F.H.A. Rummens, Can. J. Chem. 55 (1977) 3007.
[33] J. Troe, J. Phys. Chem. 83 (1979) 114.
[34] R.G. Gilbert, K. Luther, J. Troe, Ber. Bunsen Ges. Phys. Chem. 87 (1983) 169.
[35] J. Troe, V.G. Ushakov, Z. Phys, Chemistry 1 (2014) 1.
[36] J. Troe, Ber. Bunsen Ges. Phys. Chem. 87 (1983) 161.
[37] C.J. Cobos, A.E. Croce, K. Luther, L. Soelter, E. Tellbach, J. Troe, J. Phys. Chem. A 117 (2013) 11420.
[38] J. Troe, C.J. Cobos, L. Sölter, E. Tellbach, J. Phys. Chem. A (2014), in press, http://dx.doi.org/10.1021/jp501569a.
[39] C.J. Cobos, L. Sölter, E. Tellbach, J. Troe, J. Phys. Chem. A (2014), in press, http://dx.doi.org/10.1021/jp501577k.
[40] L. Zhu, W.L. Hase, A General RRKM Program (QCPE 644), Quantum Chemistry Program Exchange, Chemistry Department, University of Indiana, Bloomington, 1993.
[41] T. Beyer, E.F. Swinehart, Commun. Assoc. Comput. Mach. 16 (1973) 379.
[42] W. Forst, J. Phys. Chem. 76 (1972) 342.
[43] C. Buendía-Atencio, C.J. Cobos, J. Fluorine. Chem. 132 (2011) 474.
[44] G.Z. Whitten, B.S. Rabinovitch, J. Chem. Phys. 38 (1963) 2466.